Supporting Information

Amine functionalized MoO_3@RGO nanohybrid-based biosensor for breast cancer detection

[a]Shine Augustine, [b]Pragati Kumar, and [*a]Bansi D Malhotra

[a]Nanobioelectronics Laboratory, Department of Biotechnology, Delhi Technological University, Delhi -110042, India.
[b]Administrative Supervisor, Department of Electrical Engineering, Delhi Technological University, Delhi- 110042, India.
[*]Corresponding Author: bansi.malhotra@gmail.com

Serum samples of breast cancer patients

The serum samples of breast cancer patients were obtained from the Rajiv Gandhi Cancer Institute and Research Centre, Rohini, Delhi, (India). All the serum samples were collected under the protocol approved by the Rajiv Gandhi Cancer Institute and Research Centre Institutional Review board (RGCRIC/IRB/12/2016). Prior to collecting the serum samples, the written informed consents were taken from all the patients

We performed double antibody sandwich ELISA in anti-HER-2 coated 96 micro titter wells plate. The standard and real samples were run in triplicate followed by the colorimetric reaction recorded at 450 nm by ELISA plate reader (iMARK, Bio-rad, USA).

Figure S1

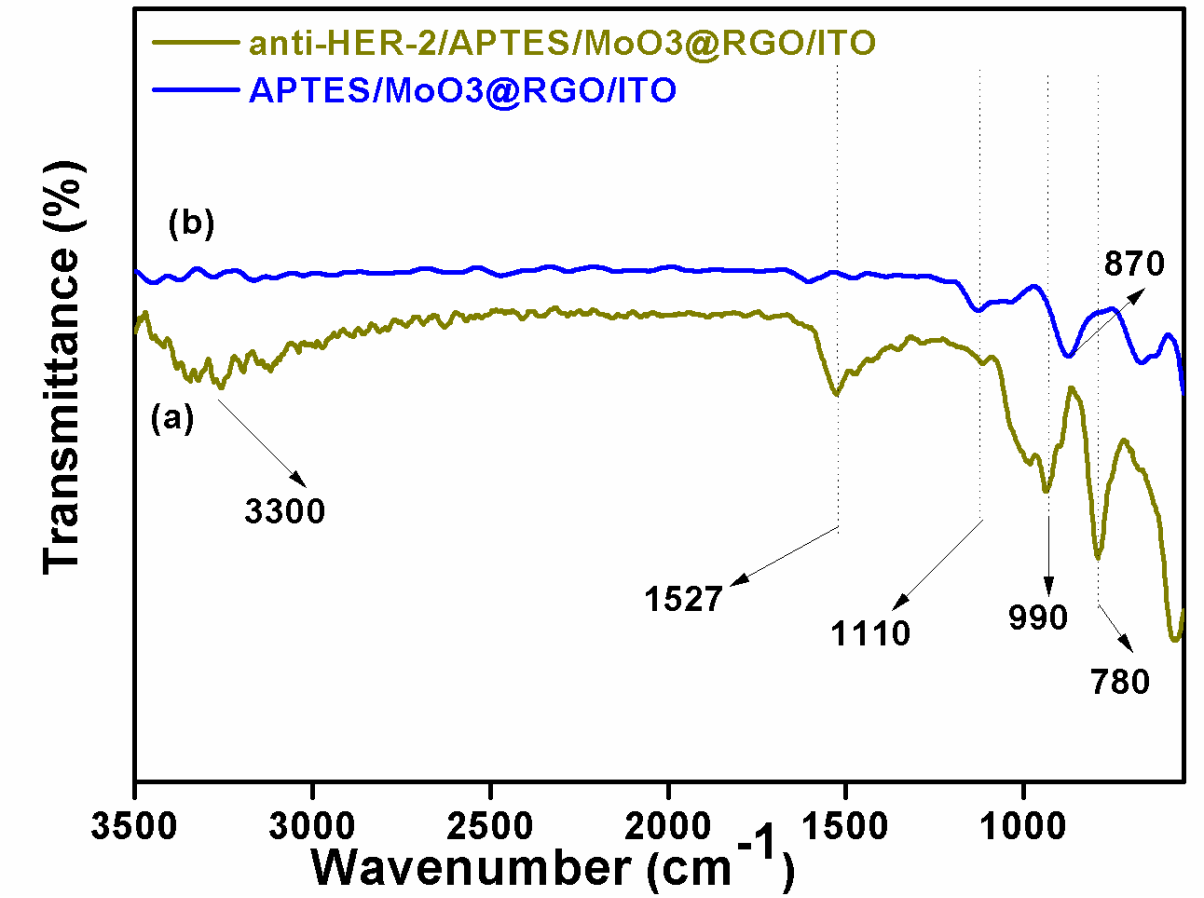

Figure S1: Fourier transform infrared spectra (FT-IR) of APTES/MoO_3@RGO/ITO and anti-HER-2/APTES/ MoO_3@ RGO electrodes**.**

Scan Rate Studies

The surface coverage of the APTES/MoO_3@RGO/ITO (Fig S2) electrode and BSA/anti-HER-2/APTES/MoO_3@RGO/ITO (Fig S3) immunoelectrode was estimated from the CV plot of I vs V using **Brown Anson Model** (Eq. S1)

$$Ip = \frac{n^2F^2\Upsilon Av}{4RT} \text{..... Eq S1}$$

Where Ip represents the peak current of immunosensor, Υ is the surface concentration of the absorbed electro-active species, F is the Faraday constant (96,485 C mol^{-1}), R is the gas constant (8.314Jmol^{-1} K^{-1}), A is the surface area of the electrode, n is the number of electrons (1) transferred, ν is the scan rate (V/s), and T is room temperature (25 °C or 298K). The surface coverage for APTES/MoO_3@RGO/ITO was found to be 4.5 ×10^{-8}mol cm^{-2} and for BSA/anti-HER-2/APTES/MoO_3@RGO/ITO was found to be and 3.9 × 10^{-8} mol cm^{-2} indicating that the BSA-anti-HER-2 interacts with the APTES/MoO_3@RGO matrix leading to reduced electron transfer.

Figure S2

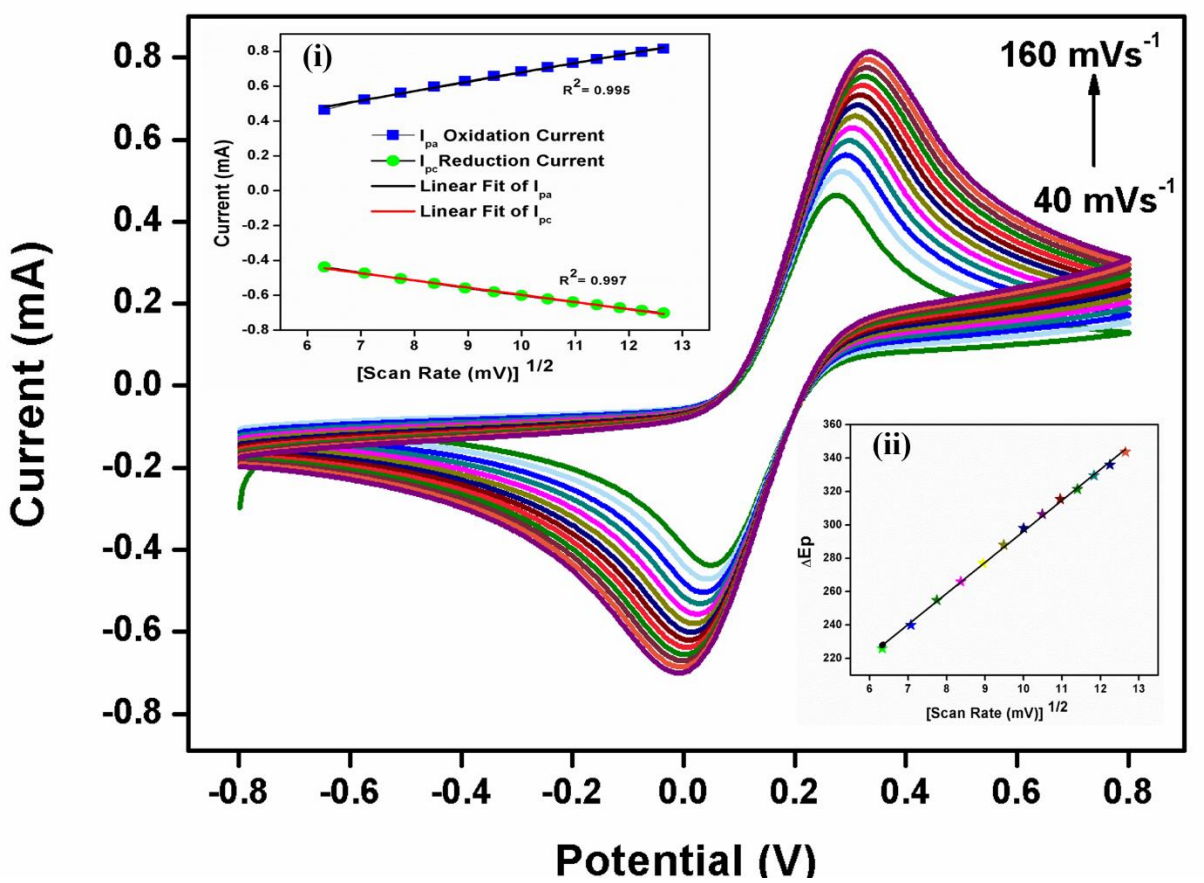

Figure S2: Scan Rate studies via Cyclic voltammetry of APTES/MoO_3@RGO/ITO (i) oxidation-reduction vs $V^{½}$ and (ii) peak potential ΔEp vs $V^{½}$.

Figure S3

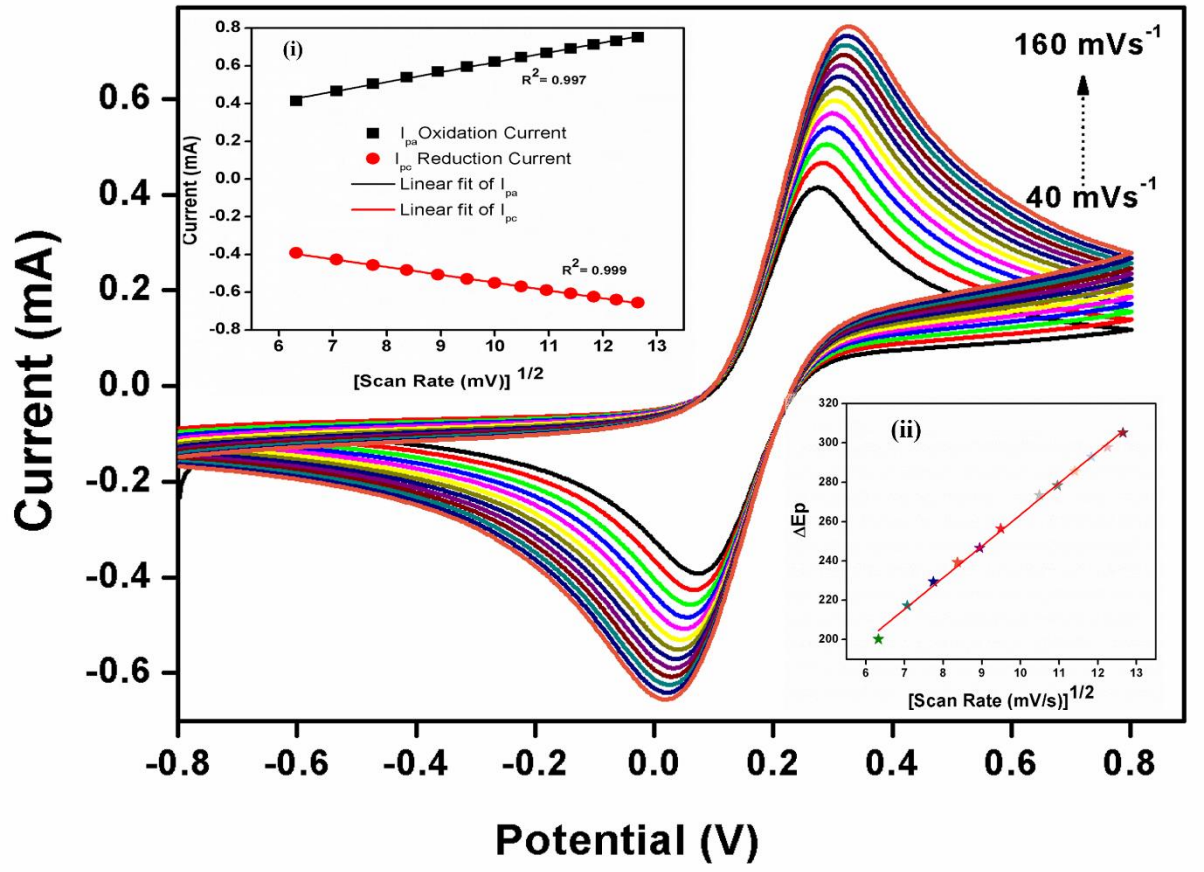

Figure S3: Scan Rate studies via Cyclic voltammetry of ITO of BSA/anti-HER-2/APTES/MoO_3@RGO/ITO (i) oxidation-reduction vs $V^{½}$ and (ii) peak potential ΔEp vs $V^{½}$.

Heterogeneous electron transfer rate (HET)

Electrochemical impedance spectroscopic measurements were conducted in the range, (0.01-100 kHz at 10 mV to investigate the heterogeneous electron transfer rate (HET) of the electrodes as shown in **Figure 8a** in the form of Nyquist Plot. The value of R_{ct} for APTES/RGO/ITO, APTES/MoO_3/ITO and APTES/MoO_3@RGO/ITO were determined to be 900 Ω, 1.09 kΩ and 709.13 Ω, respectively. The HET coefficient (K_0) calculated using the equation Eq. S2

$$K_0 = RT/n^2F^2A\,R_{ct}C \text{……. Eq. S2}$$

Where F is the Faraday constant, A is the active surface area of the electrode, T is temperature, R is the molar gas constant, n is the number of electrons (n = 1), C is the concentration of the electroactive species, and Rct is charge transfer resistance of electrode surface. The equvivalent

circuit model is shown in Figure 8a inset (i). Rs depicts the solution resistance, Rct is the charge transfer resistance, C_{dl} is the double layer capacitance and W is the warburg impedance. The HET rate in case of APTES/MoO_3@RGO/ITO was found to be the highest (3×10^{-7} cm s^{-1}) with respect to APTES/MoO_3/ITO (1.9×10^{-7} cm s^{-1}) and APTES/RGO/ITO (2.3×10^{-7} cm s^{-1}). This may be due to the synergistic effect of the synthesized nanohybrid, which imparts a better electron transfer and the presence of RGO provided better electrocatalytic activity leading to the smooth conduction of electrons.

Figure S 4

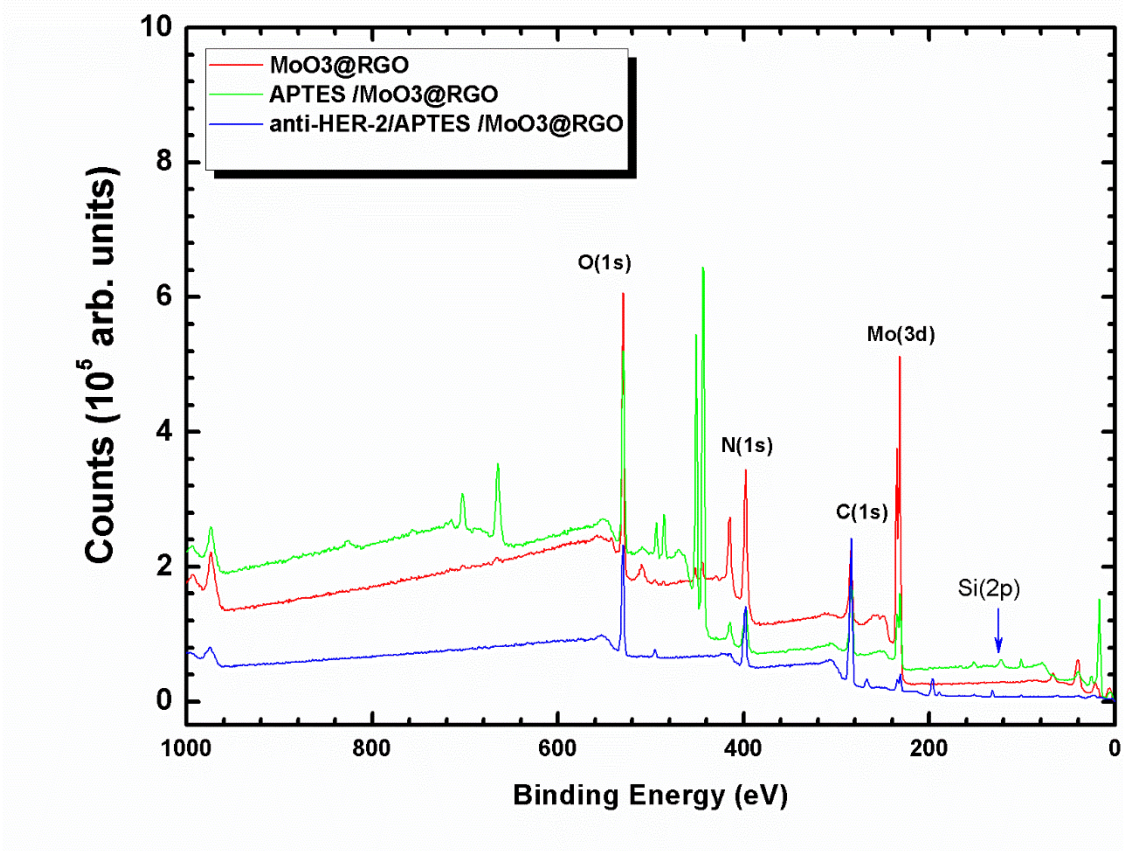

Figure S4 : The survey scan spectrum of the MoO_3@RGO, APTES/MoO_3@RGO/ITO and anti-HER-2/APTES/ MoO_3@RGO/ITO.

Detection of breast cancer biomarker (HER-2)

The limit of detection of the fabricated sensor was determined using the following equation

$$Limit\ of\ detection = k \times \sigma / sensitivity\ (m) \ldots\ldots\ldots\ldots\ldots\ldots\ldots \quad (Eq.\ S3)$$

with k is the confidence level of parameters (k =3 with a statistical confidence of 99.6 %), σ is the standard deviation of the blank signal (taken for 5 repeated measurements). The limit of detection of this immunosensor was calculated to be 0.00 1 ng mL^{-1}.

Figure S5

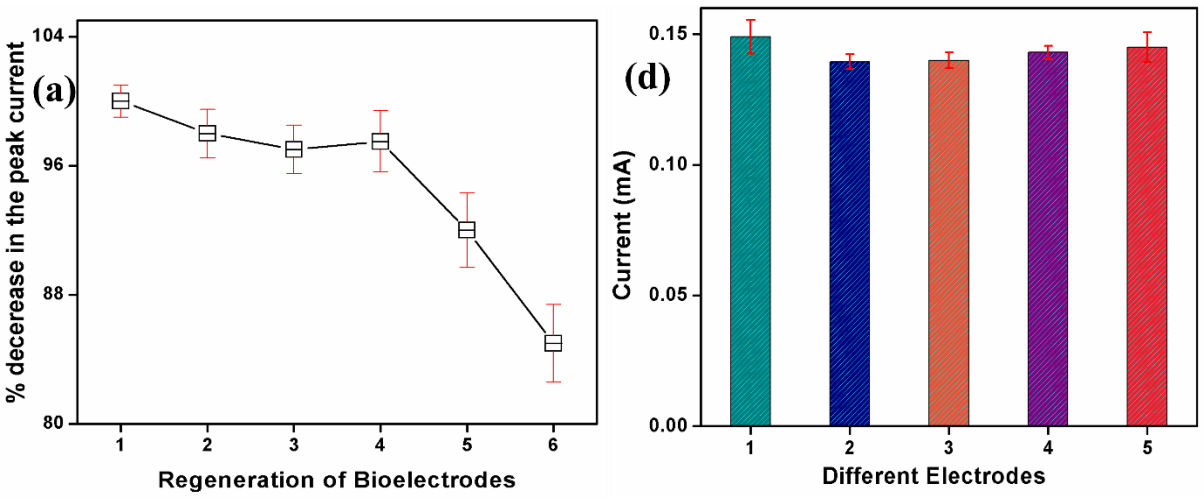

Figure S5: (a) Regeneration studies (b) Reproducibility studies of five different electrodes of BSA/anti-HER-2/APTES/MoO_3@RGO/ITO.

Figure S6

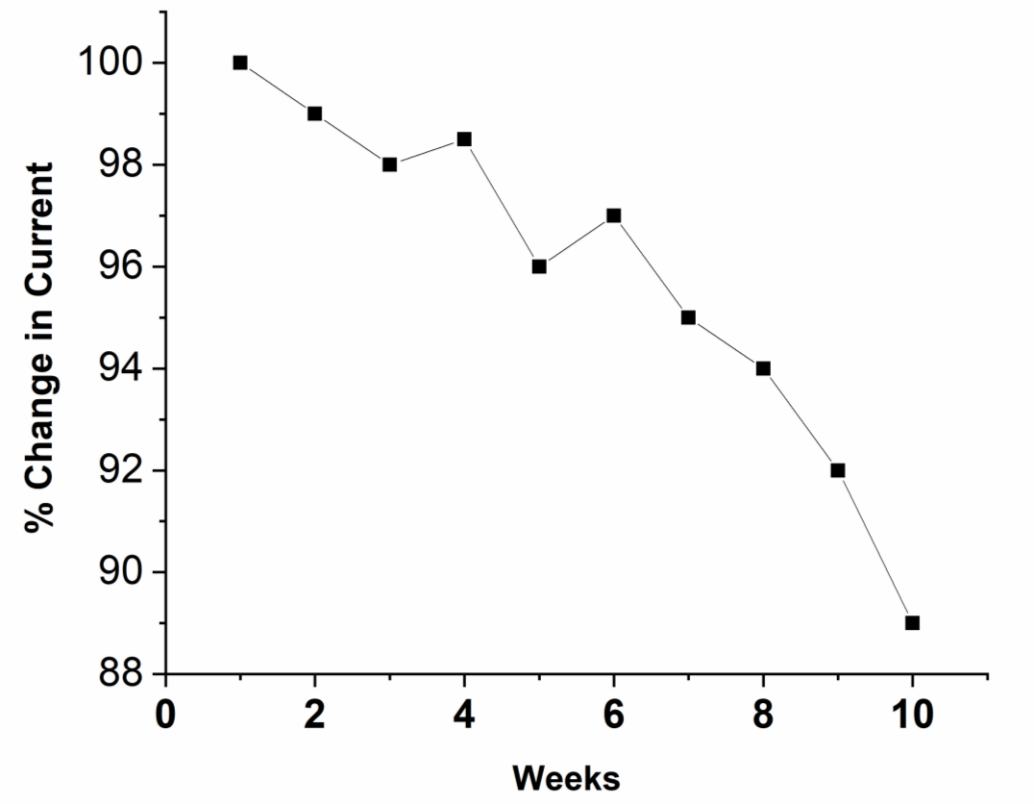

Figure S6 : Shelf Life of the fabricated immunoelectrode determined by DPV (BSA/anti-HER-2/APTES/MoO_3@RGO/ITO) at regular intervals for 10 weeks

Figure S7

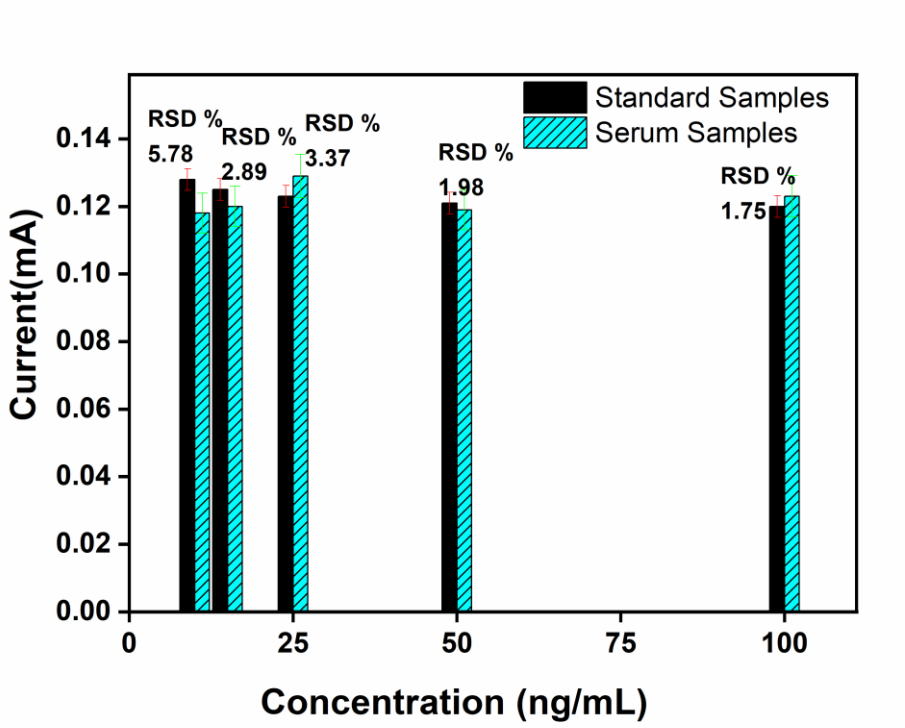

Figure S7: % RSD of HER-2 concentration in serum samples using BSA/anti-HER-2/APTES/MoO_3@RGO/ITO immunoelectrode with the standard ones

TABLE S1: Determination of % RSD of HER-2 concentration in serum samples using BSA/anti-HER-2/APTES/MoO_3@RGO/ITO immunoelectrode with the standard ones.

S.No.	HER-2 concentration (ng mL^{-1}) determined through ELISA	Value of Current obtained with Serum Sample (mA)	Value of Current obtained with Standard Sample (mA)	% Relative Standard Deviation
1	10	0.128	0.118	5.78
2	15	0.125	0.121	2.89
3	25	0.123	0.129	3.37
4	50	0.121	0.119	1.98
5	100	0.120	0.123	1.75